THE STATUS OF THE TEVATRON COLLIDER

J. Peoples

Fermi National Accelerator Laboratory*
Batavia, Illinois 60510

In the initial but preliminary agenda for this conference my talk was included in the session entitled Near Future and Future Physics. This agenda seemed quite reasonable to me because a largely constructed but uncommissioned collider seemed to be an appropriate subject for the Near Future. The SSC certainly belongs to the Future. One aspect of such a talk, is the content is not constrained by the reality of results. In the minds of experimenters, and I am sometimes in their number, the colliders of even the Near Future will be colliding at their design luminosities with negligible down time for failures. The detectors of the Future have no dead zones or dead times. The energy resolution and spatial resolution may not even be limited by ISAJET. Not even the most optimistic perception of technology will slow the data taking rate. While the reality of the Tevatron collider run in the fall of 1985 is a constraint on any exaggerations that I might be tempted to make, I approached the talk expecting to be one of several speakers proclaiming the rosiest future.

*Operated by Universities Research Association Inc., under contract with the United States Department of Energy

When I read the actual program for the meeting a few days ago I was surprised to find that my talk was at the end of a long session devoted to the presentation of real collider data. I wondered whether the program committee was suggesting that I merely show an event or two from the 27 events accumulated early in the morning of October 13, 1985, and then let the weary audience scatter to the restaurants of Chicago. I consulted a member of the program committee for advice. He responded, "two thirds physics and one third accelerator". Thus I will now show two events, and one picture of the Accelerator.

The part of my talk devoted to experimental results is now complete. Let me now turn to promising Fermilab's very Near Future in order to give a sense of what I believe is possible. I will give you a brief description of the Tevatron, a status report on its performance to date, and a status report on the experiments which are under construction.

Tevatron Collider

The two most basic design parameters of a collider are its center of mass energy and its luminosity. The Tevatron design goals for these parameters are 2000 GeV and $10^{30}cm^{-2}sec^{-1}$ respectively.[1] When the Tevatron reaches this level of performance it will permit the exploration of mass scales extending up to 500 GeV/c^2. A more complete set of design parameters of the Tevatron Collider is given in Table 1.

The design luminosity is achieved when three bunches of protons and three bunches of antiprotons with the characteristics given in Table 1 circulate in opposite directions in the Tevatron. The bunches are spaced so that collisions occur at AØ, BØ, CØ, DØ, EØ, and FØ. The CDF detector is located at BØ. Three smaller experiments are located at DØ, CØ, and EØ. Eventually, in 1989, the DØ detector will be located at DØ. Except for CDF, each experiment must share the straight section with accelerator equipment. Because there are two accelerators in the same enclosure, the Main Ring and the Tevatron, the space was already very congested without the presence of experiments. Since the experimenters had an irrepressible desire to do experiments, a way was found to fit four experiments into the Main Ring enclosure.

Although most of the accelerator portion of this talk will be devoted to describing how we plan to accumulate $2x10^{11}$ antiprotons and then put them into three antiproton bunches with the properties given in Table 1, I will start with the sequence of steps which results in the preparation of dense proton bunches in the Tevatron.

Protons are accelerated in turn by the ion source, the Linac and the Booster, the three accelerators which constitute the Injector. While protons are being accelerated in the Booster they consist of a train of 84 bunches separated from one another by 5.65 m. This bunching is preserved when the protons, upon reaching a kinetic energy of 8 GeV, are transferred to the Main Ring and they remain bunched throughout the acceleration cycle in the Main Ring. When protons are accelerated for the purpose of forming a single bunch of $6x10^{10}$ protons in the Tevatron only four to five adjacent bunches are extracted from the Booster and injected into the Main Ring at AØ. The remaining bunches are extracted and sent to the AP-4 dump. After the bunches have been

Table 1: Tevatron Collider Design Parameters.

Center of Mass Energy	2000 GeV
Luminosity	$10^{30} cm^{-2} sec^{-1}$
Number of protons per bunch	6×10^{10}
Number of antiprotons per bunch	6×10^{10}
Number of proton-antiproton bunch pairs	3
Normalized transverse emittances of Protons and antiproton (95%)	24π mm-mr
Revolution frequency	49×10^{3} Hz
Beam Life time	>12 hours
Maximum Antiproton Accumulation Rate	10^{11} hr^{-1}
Collection time	5 hours

A schematic layout of the Tevatron is shown in Figure 1.

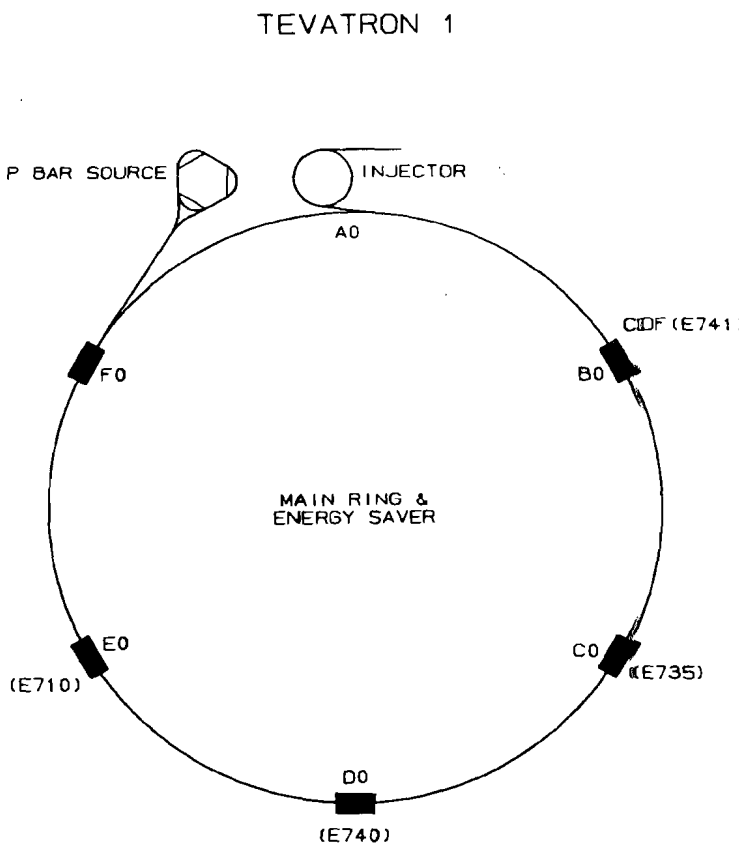

Figure 1 - A schematic representation of the Fermilab Collider and the accelerators which create a proton and antiproton beam. The numbers in parenthesis designate colliding beam experiments.

accelerated to 150 GeV, they are coalesced into a single bunch. The extra step of coalescing 4 to 5 bunches into a single bunch is necessary because it is not possible to accelerate bunches of $6x10^{10}$ protons through the Main Ring transition energy without excessive losses. It is possible to accelerate bunches of $2x10^{10}$ or less with only a small loss. Once a single bunch has been formed it is transferred to the Tevatron. The bunches remain in the Tevatron at 150 GeV until all of the protons and antiproton bunches have been injected into the Tevatron. After this step is complete the ensemble of six bunches is accelerated to the final energy.

While it is difficult to pack $6x10^{10}$ protons into a single bunch with the phase space volume defined by the emittances in table 1, it is much more difficult to put $6x10^{10}$ antiprotons into a single bunch with the same phase space volume. To give you a flavor of that difficulty let me present a very brief description of the Antiproton Source, starting with the process of antiproton production and accumulation. A schematic layout of the Antiproton Source is shown in Figure 2.

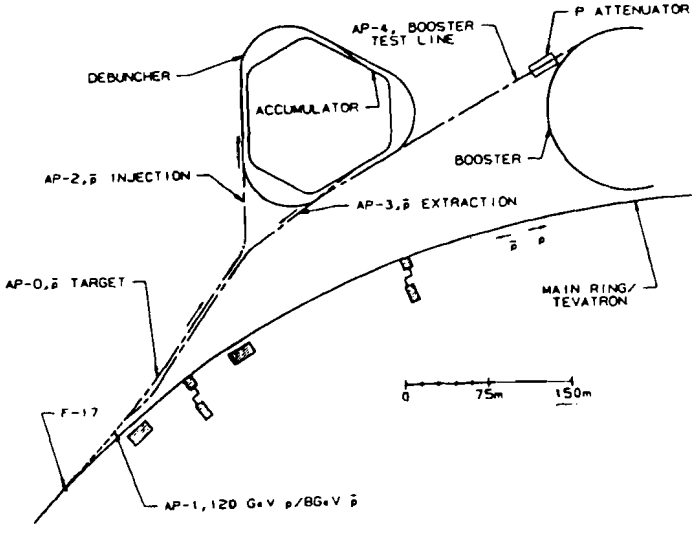

Figure 2 - Schematic of the antiproton source and the related accelerators and beam transport lines used for pbar production and source commissioning.

Antiproton production is initiated by accelerating a full Booster batch consisting of 84 proton bunches to 120 GeV in the Main Ring. After reaching this energy the bunch widths are made very narrow by a bunch rotation and then the batch is extracted at F17 and transported to a target at AP-0. 8.89 GeV/c negative secondaries contained within a fractional energy spread of 3.5% are collected and transported to the Debuncher along the AP-2 line. The number of antiprotons captured in the Debuncher is proportional to the fractional energy spread which the Debuncher can accept as well as the size of its aperture. As the name implies the beam is debunched with the rf in such a way that the longitudinal emittance, ϵ , is preserved. Since it is just the product of the energy spread, ΔE, and the time spread, Δt, the energy spread decreases as the time spread increases. The objective of debunching is to make the energy spread as small as possible since the microwave output power required to cool the antiprotons is proportional to $(\Delta p)^3$. Since the time spread can only be increased until the bunches just touch, it follows that Δt of the antiproton bunches should be as small as possible when they enter the Debuncher. The antiproton bunch widths can be minimized by minimizing the proton bunch width just before extraction. This is done by subjecting the protons to a bunch rotation just before extraction. As soon as the antiproton bunches are injected into the Debuncher they are debunched by a bunch rotation. This is followed by adiabatic debunching of the rotated bunches thereby reducing the energy spread from 3.5% to .22%. This process takes about 10 ms.

The antiprotons are then stochastically cooled in order to reduce the transverse emittances of the antiproton beam.[2] The cooled antiprotons can then be transferred to the Accumulator without significant loss and the production cycle begins again.

Roughly 5000 batches of antiprotons need to be collected and cooled in the Accumulator before there are sufficient antiprotons to provide a fill for colliding beams. In order to accumulate each batch without driving the previously accumulated batch out of the Accumulator it is necessary to inject a batch of antiprotons, move it to the edge of the stack of previously collected antiprotons, and then cool the fresh batch into the stack. The last step provides the room in phase space to inject the next batch. This sequence takes advantage of the fact that antiprotons of slightly different momenta can be physically separated from one another in regions of high dispersion. Figure 3, which shows the radial distribution of antiprotons in a high dispersion region during each step of the stacking process illustrates how this is done. A batch of antiprotons with a momentum of 8.89 GeV/c is injected into the accumulator. When these antiprotons traverse the high dispersion straight sections at A20, A40, and A60, they will be displaced radially outward from the center of the aperture by 65 mm because their energy is 70 MeV higher than the energy of the central orbit as shown in figure 3a. The fresh batch of antiprotons is adiabatically captured by the h=84 rf system. Because the momenta of antiprotons in the stack are at least 70 MeV less than the antiprotons on the injection orbit, the antiprotons in the stack are not captured by the rf. Once the antiprotons are captured they are decelerated toward the stack edge as shown in figure 3b. Since the antiprotons in the stack were not captured initially they will not be decelerated although their energy varies slightly with time because of the rf voltage. In fact the antiprotons at the high energy edge of the stack will be phase displaced to a higher energy as the rf bucket moves to the edge of the stack. As the antiprotons approach the edge of the stack the rf voltage is reduced to zero thereby debunching the captured beam. As soon as the rf voltage is off the stack tail momentum cooling system is turned on. This sequence of steps requires

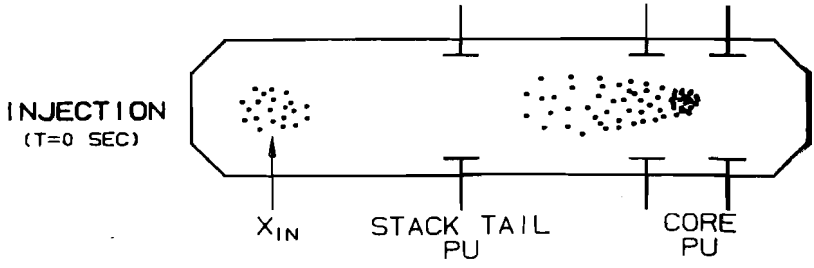

Figure 3a

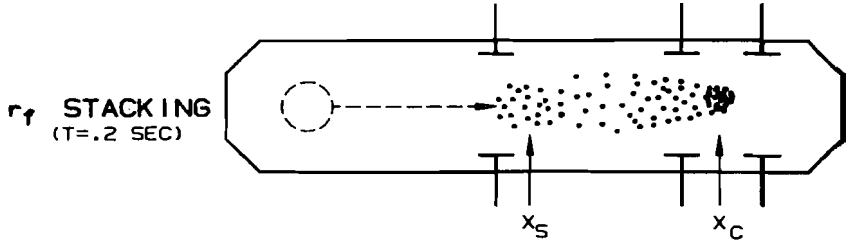

Figure 3b

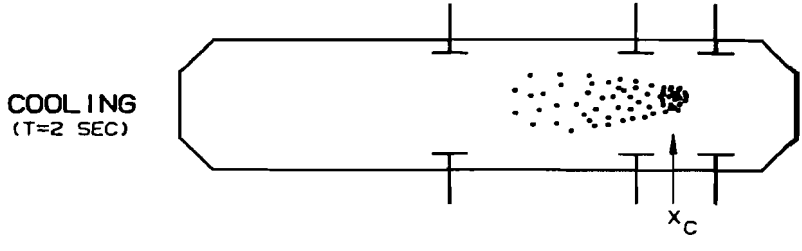

Figure 3c

Figure 3 - Radial distribution of beam in a high dispersion straight section during each step of stacking process. Beam from the Debuncher is injected at X_{in} (3a). After rf capture it is moved to the edge of the stack X_s, just beyond the stack tail momentum pickups (3b). The antiprotons are decelerated by the stack tail cooling system toward the core, X_c (3c).

about .2 seconds, leaving 1.8 seconds or more for cooling. The stacktail momentum cooling system causes each antiproton to be slowly decelerated toward the core as shown in Fig. 3c. Since the sensitivity of the pickups is an exponentially decreasing function of the distance from the stack tail pickups, on average each antiproton is decelerated by a smaller amount on successive turns. This causes the number of antiprotons per unit energy to increase as their energy approaches the energy of the core. Typically the antiprotons at the edge of the stack are decelerated by 20 MeV in the remaining 1.8 sec thereby clearing the edge of the stack tail of particles. The time that it takes for the antiprotons to migrate from the stack edge to the center of the core approaches four hours once the core contains 4×10^{11} particles. Figure 4 shows the number of antiprotons per unit energy, $\psi(E)$, at a succession of different times.

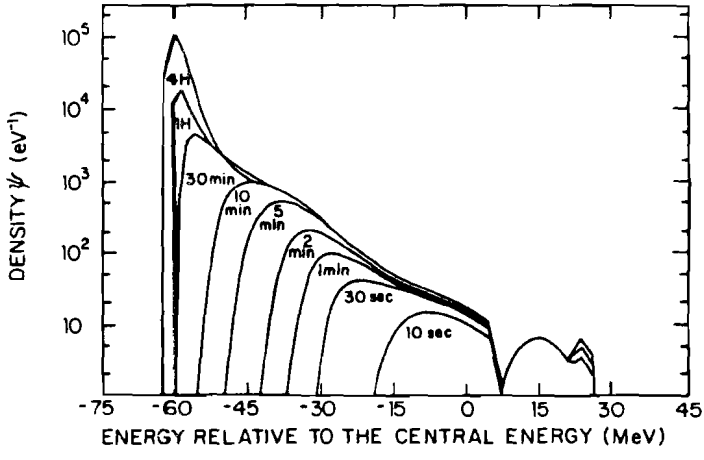

Figure 4 - Antiproton distribution in the Accumulator as a function of time when 7×10^7 antiprotons are injected into the Accumulator every 2 seconds.

The design parameters of the Antiproton Source are given in Table 2.

Table 2 - Antiproton Source Design Parameters

120 GeV proton cycle time	2.25 sec
120 GeV proton intensity/cycle	2×10^{12}
Debuncher fractional momentum acceptance	3.5%
Debuncher aperture in both planes	20π mm-mr
Antiprotons stored in the Debuncher/cycle	7×10^{7}
Fraction momentum spread after debunching	.22%
Debuncher emittances ϵ_r, ϵ_v (95%) after cooling	5π mm-mr
Accumulator fractional momentum acceptance	2.0%
Accumulator momentum acceptance (injection orbit)	.3%
Accumulator vertical aperture,	10π mm-mr
Antiprotons transferred to $\bar{p}$ stack/cycle	6×10^{7}
Peak antiproton accumulation rate	10^{11}/hour
Peak density in the core when 5×10^{11} antiprotons are in the core	10^{11}/MeV
Emittances ϵ_r, ϵ_v (95%) of the core	$<2\pi$ mm-mr

Once the density of antiprotons in the core reaches 10^{11}/MeV and the transverse emittances are 2πmm-mr or less, the transfer sequence which will ultimately result in a single bunch of 6×10^{10} antiprotons in the Tevatron is initiated. The sequence is not initiated until the Tevatron is filled with the appropriate number of proton bunches as described earlier.

The first step in the antiproton transfer sequence is to form a single bunch containing 8×10^{10} $\bar{p}$'s with an h=2 suppressed bucket system. The rf frequency is h times the revolution frequency. Initially the bunch length is about 240m long. Once formed it is accelerated to the accumulator extraction orbit, and

then compressed to a length about 50m by a second h=2 system. Finally it is rebunched with a 53 MHz, h=84 system into 7 to 8 bunches, each of which is about 1 m long. The last step is done with a third rf system, the same one which was used for stacking. The $\bar{p}$'s are extracted and transferred to the Main Ring where the 7 to 8 bunches are captured by the 53 MHz rf system of the Main Ring. From this point on the process is the same as the process of accelerating and coalescing proton bunches described earlier. The 7 to 8 bunches of antiprotons are accelerated from 8GeV to 150GeV and then coalesced into a single bunch. The coalesced bunch is then transferred to the Tevatron. This step is repeated two more times.

At this point there are 3 bunches of protons and 3 bunches of antiprotons circulating in the Tevatron at 150 GeV. The relative locations of the proton and antiproton bunches are adjusted by changing the energy of the pbars with respect to the protons so that one group of particles trasverses the ring faster than the other. The location of an antiproton (proton) bunch relative to an other antiproton (proton) bunches can only be adjusted before each antiproton (proton) bunch is extracted from the Main Ring. The process of synchronizing the position of a bunch in the Main Ring with a bunch in the Tevatron is called cogging. The whole ensemble of bunches is then accelerated to an energy of 900 GeV or more. The low β magnets are energized thereby reducing β^* to 1 m. Once the collisions occur in the right place the proton and antiproton energies are made the same thus keeping the collision location fixed. Since BØ is the only collision region with a low beta insertion the value of β^* at the other collisions points remains between 80 and 100 m.

Tevatron Status

Let me now describe the status of the Tevatron and how well we have done toward reaching our design goals.

The Tevatron and the Pbar Source were operated as a single system just for a few hours last October. It was during that run that the 27 events were observed. Their combined performance during that run is given in Table 3.[3)]

Table 3: Performance of the Tevatron in October 1985

Peak luminosity	$2 \times 10^{24} cm^{-2} sec^{-1}$
Peak center of mass energy	1600 GeV
Protons/bunch	4×10^{10}
Antiprotons/bunch	3×10^{6}
Number of bunch pairs, Nb	1
Invariant emittances, ϵ_n^x, ϵ_n^y	50π mm-mr
$\beta*$ at BØ	1 m
Pbar accumulation rate	10^9 hr-1

We are not too concerned with the fact that the luminosity was nearly a factor of a million below the design, since the purpose of the test was to integrate all of the systems and identify the inevitable list of problems which occur when a system as complex as this is tried for the first time. While there were no insoluble problems there were a lot of soluble ones. During the past year we made many small improvements which should lead to a significant improvement in the luminosity.

While these improvements were being made the primary activities were the construction of the Main Ring overpass at BØ and the DØ experimental area. The demolition of the Main Ring tunnel at DØ and BØ was postponed until October 14, 1985 in order to carry out the colliding beams test. The vertical separation between the Tevatron and the Main Ring was increased to 6m at BØ thereby allowing the Main Ring beam to pass over the entire CDF detector. Since such a large vertical distortion cannot be done abruptly it extends over 500m of the Main Ring circumference. It was necessary to excavate the earth away from the Main Ring tunnel

enclosure and then rebuild the enclosure to accommodate the new location of the Main Ring, while preserving the location of the Tevatron. The BØ overpass including the reinstallation of the Main Ring and the Tevatron was completed in July of 1986.

The construction of the DØ Experimental Area was started in August of 1985. The Collision Hall including the shielding wall which isolates the Tevatron and Main Ring beams from the adjacent assembly area was completed at the end of August of 1986, thereby allowing us to resume accelerator operations. Commissioning has now been underway for two weeks. Although our progress has been excellent, a number of problems associated with the overpass need to be solved before the Main Ring is ready to fulfill its role in collider operations.

The Tevatron is operational again and protons were stored recently at 900 GeV. The prospect of being able to run at 900 GeV/beam in the fall is very good.[4)]

Pbar Source Status

Pbar Source operations have been in progress intermittently since February 1, 1986 when the AP-4 test beam from the Booster to the Debuncher was commissioned. Measurements of the stacking rate using protons from the Booster have demonstrated that with an average rate of one pulse of 5×10^{7} 8 GeV protons every 3 seconds a stacking rate of 1.5×10^{10} protons/hour can be sustained. The stacking efficiency was only 50% because of betatron heating caused by the stack tail momentum system. Measures are now being taken to eliminate this problem. Once this is done the Accumulator will be capable of stacking in excess of 3×10^{10}/hour. A density of 4×10^{10} protons/MeV in a core of 2×10^{11} protons has been achieved. A summary of the current status of the Debuncher and Accumulator performance using Booster protons is given in Table 4.

Table 4: Pbar Source Performance with Protons
(October 1986)

Debuncher fractional momentum acceptance	3.5%
Debuncher horizontal and vertical aperture	20π mm-mr
Debuncher emittance after cooling 7×10^{7} for 2 sec	5π mm-mr
Accumulator momentum acceptance (injection orbit)	.3%
Accumulator vertical aperture	8.5π mm-mr
Accumulator horizontal aperture at injection	11π mm-mr
Peak (proton) accumulation rate	1.5×10^{10} hr-1
Peak density in the core when 2×10^{11} protons are in the core	4×10^{10} (mev)-1
Emittance ϵr, ϵv, (95%) of the core	1π mm-mr

Antiproton production has not been resumed because the polarity of the magnetic field of the Debuncher and Accumulator is set for protons. This allows us to take advantage of the relative ease of commissioning the source with protons from the Booster while the Main Ring is being recommissioned. Since the number of secondary 8.89 GeV/c protons produced by targetting 120 GeV primary protons at AP-0 and subsequently captured in the Debuncher is a very good predictor of $\bar{p}$ production rates, measurements of secondary protons yields have been made. They verified that the improvements made to the Debuncher aperture, made during the spring of this year increased the acceptance by a factor of 3. This was expected since the Debuncher aperture was only 10π mm-mr x 12π mm-mr in October of 1985. An additional factor of 1.5 was obtained by eliminating an aperture restriction in AP-2. Taken together these improvements should provide a factor 5 increase in the $\bar{p}$ accumulation rate. During the October of 1985 test, the Main Ring cycle time was only 5 seconds. It can be reduced to 2.5 seconds once routine collider operation begins. We expect that the accumulation rate will be a factor of ten larger than it was in October of 1985 after stacking beam becomes routine. The commissioning of the cooling systems should be sufficiently advanced by November 1 to permit us to reverse the polarity of the magnets and begin $\bar{p}$ accumulation. The projected performance of the Pbar Source should allow us to

achieve a luminosity of 10^{29} cm^{-2} sec^{-1} toward the end of the collider run. Speaking from the parochial perspective of the Accelerator Division we hope that this run will start in January and last for three or four months thus allowing us to accumulate an integrated luminosity of 100 nb^{-1}, the fondest wish of the experimenters.

Tevatron Collider Experimental Program

When the colliding beam run begins four experiments will be ready to observe the collisions. Table 5 shows the approved experiments by number, the subject of their investigation, and their location.

Table 5: Tevatron Collider Experimental Program

Experiment Number	Subject	Location
E710*	Elastic Scattering & total cross section	EØ
E713+*	Search for monopoles & & other heavily ionizing particles	DØ
E735*	Search for evidence of a quark-gluon plasma phase transition	CØ
E740 "DØ"	Physics at the electroweak scale	DØ
E741* "CDF"	Physics at the electroweak scale	BØ

*Scheduled to take data during the 1986-1987 running period.
+After 86-87 the DØ straight section will be used by E740, "DØ".

E710: Bologna, Cornell, Fermilab, Maryland, George Mason, Northwestern

The objective of E710 is to measure the $p\bar{p}$ elastic scattering and total cross sections in the range of 150 to 1000 GeV per beam. While most of the collider running time will be dedicated to running at the highest energy, brief periods of lower energy running will occur once stable operation has been achieved. A schematic layout of the experiment is show in figure 5.

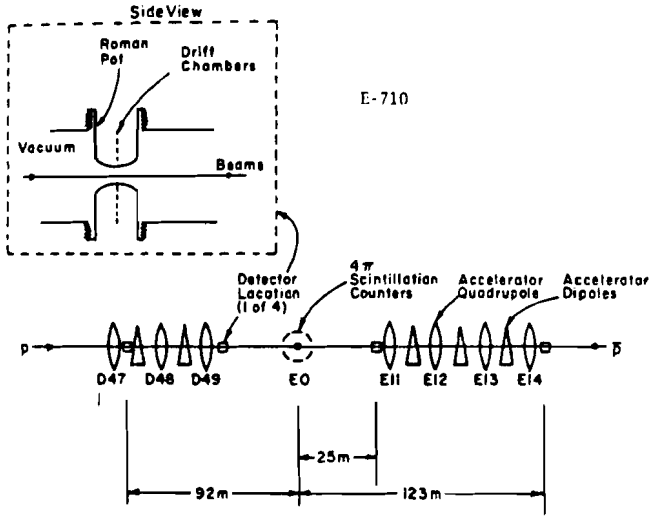

Figure 5 - Schematic layout of E710.

$\bar{p}p$ elastic scattering events are measured with drift chambers mounted inside Roman pots at 2 locations on both sides of the interaction region. At 1000 GeV per beam these detectors can detect scattered protons and antiprotons if the momentum transfer, Q^2, is greater than 4×10^{-3} $(GeV/c)^2$ and less than 1 $(GeV/c)^2$. The experimenters measure the yield of elastically

scattered events, $\Delta Ne(Q_i^2)$, in the Q^2 interval of Δ_i^2 centered at Q_i^2. If the efficiency for detecting events at Q^2 is $E_e(Q^2)$, then the cross sections are related to luminosity and yield by (1) and (2).

$$\frac{d\sigma e}{dQ^2} = \frac{\Delta Ne(Q_i^2)}{\Delta Q_i^2} [Ee(Q_i^2) \int L\bar{p}pdt]^{-1} \quad (1)$$

$$\sigma_e = \sum_{\Delta_i^2} \Delta N_e(Q_i^2) [E_e(Q_i^2) \int L\bar{p}pdt]^{-1} \quad (2)$$

Inelastic events are concurrently observed by detecting the charged particles produced in beam-beam collisions which either transverse a box of scintillating counters that covers nearly all of the interaction region except for the 10 cm diameter vacuum pipe or a set of ten ring counters, five on each side of the interaction region. Although these counters are not shown in figure 5 they are located within ±25 m of the interaction point. The furthest downstream of these ring counters subtends a minimum angle of 2.7 mr. Since most high energy particles emerging from elastic events and low mass diffractive events will not be detected by these downstream counters, detectors are placed in Roman Pots on each side of the interaction region 25 m from the interaction point. Once the protons and antiprotons have been stored these detectors can be moved closer to the circulating beam and detect elastically scattered protons which have $Q^2 < 1(\mathrm{Gev/c})^2$ as well as most inelastically scattered protons. A second set of detectors are mounted in another set of Roman Pots deep in the machine, 90° in betatron phase advance from the intersection region on either side of the interaction region. These are used to detect the low Q^2 elastically scattered events. The combined detection efficiency of all of these detectors for inelastic events, E_i, is ~98%. The inelastic events, N_i, are related to the inelastic cross section, σ_i, the efficiency, and the integrated luminosity by (3).

$$\sigma_i = N_i [E_i \int L\bar{p}pdt]^{-1} \tag{3}$$

$d\sigma_e/dQ^2$ can be written as a hadronic part, a Coulomb part and a interference term as follows:

$$\frac{d\sigma e}{dQ^2} = \frac{\sigma_T^2}{16\pi}(1 + |\rho|^2)(\exp-bQ^2) + \frac{4\pi\alpha^2}{Q^4} + \left(\frac{2\sigma_T\sqrt{\pi\alpha}}{Q^2}\right)\rho\exp-(bQ^2/2) \tag{4}$$

Since σ_T is the sum of σ_i and σ_e it is possible to determine σ_T and the luminosity from the measurements provided the efficiencies are known.[5] The efficiencies are determined by a straight forward calculation.

The term proportional to σ_T^2 can be extracted from the data since it is a slowly varying function of Q^2 for $Q^2 > .02$. Since ρ, the ratio of the real to imaginary part of the nuclear scattering amplitude, is expected to be about 0.1 the uncertainty in $|\rho|^2$ is smaller still and thus it does not introduce a significant error in the determination of the total cross section. The data between $.002<Q^2<.02$ can be used to determine ρ to a precision of 15% to 20%.

Because the beam size is proportional to the square root of the emittance the beam emittance is one of the limitations to the measurement of Q^2. The detectors cannot be moved into the tails of the beam without significantly reducing the beam intensity. It follows that there is a distance of closest approach. The experimenters believe that they can bring the detectors to within 5 mm of the beam centers after the beams have been accelerated to 1000 GeV. If they are able to do this they will reach Q^2 as small as .004 $(GeV/c)^2$. Since the coulomb-nucleon interference

has its maximum value at Q^2=.001, the experiment will be sensitive to the pure coulomb amplitude for beam momenta below 500 GeV. At these momenta the efficiency of the detector can be calibrated absolutely.

The luminosity at EØ will be nearly one hundred times smaller than at BØ since β_T^* and β_V^* are roughly 80 meters. Because the cross sections of interest are greater than 1 mb this is not a problem.

This method of obtaining the elastic and total cross sections was successfully used at the Sp$\bar{p}$S.[5] It is worth noting that the results of this experiment will allow other Tevatron experiments to use elastic events and the inelastic events as a luminosity monitor.

The installation of E710 is in progress. All of the insertions into the Tevatron are complete. The experiment should be ready for beam in January.

E735: Duke, Fermilab, Iowa State, Notre Dame, LLL, Purdue, Wisconsin[6]

The goal of the experiment is to search for evidence of a quark gluon plasma created in $\bar{p}$p collisions. In order for experimental observables, such as multiplicity, momenta, and particle type, to reveal the plasma a number of assumptions must be made. First the subset of $\bar{p}$p collisions in which a plasma of quarks, antiquarks and gluons is created must not be rare. Second the quarks and gluons must come into thermal equilibrium before they materialize as hadrons so that the language of thermodynamics is appropriate. If these conditions are applicable then the following physical picture is at least plausible. As the energy per unit volume in a proton (or antiproton) increases as a result

of the collisions, the energy per degree of freedom in the "normal degrees" of freedom of the proton will increase until some of the quarks, antiquarks, and gluons which are formed by the collision are sufficiently energetic to act like free particles within the interaction volume. As the energy per unit volume increases further the energy will go into increasing the number of degrees of freedom as manifested by the number of quark-antiquark pairs and gluons. The energy per degree of freedom should remain roughly constant until all the degrees of freedom are excited or at least until it is more probable to add more energy to some degrees of freedom than it is to create new degrees of freedom. The transition from "normal" hadronic matter to a plasma of quarks and gluons can be thought of as a phase transition. The issue confronting the experimenters is whether there is a large enough subset of soft collisions in which enough of the longitudinal energy is deposited in a small enough volume to create a quark-gluon plasma which can be distinguished from the background of other final states. As in all investigations of hadron collisions one cannot investigate the behavior of quarks and gluons directly. One must observe hadrons, the quark and gluon states which are color neutral.

If N_c denotes the charged particle multiplicity, and y the rapidity, then dNc/dy near y=0 should be proportional to the number of quark, antiquark, and gluon degrees of freedom excited by the collision. Assuming that all transverse degrees of freedom are in thermal equilibrium near y=0 the average transverse momenta of the soft particles, $\langle P_T \rangle$, should be proportional to the energy per degree of freedom. The quark gluon plasma will be observable only if the multiplicity is much larger than the normal multiplicity, since this description is plausible only in the limit of a large number of degrees of freedom.

If dNc/dy shows a distinct step as a function of $\langle P_T \rangle$ then it can be interpreted as a phase transition.[7] Since the number of free quarks and antiquarks in the deconfined phase should be much larger than in ordinary collisions, one might also expect to see a sharp increase in the production cross section of low mass e+e- pairs as a function of $\langle P_T \rangle$. Since gluons are flavor neutral a phase transition could also be revealed by an increase in low energy $K^+ K^-$ pair production.

To make these observations the experimenters are constructing a detector, the plan of which is shown in Figure 6.

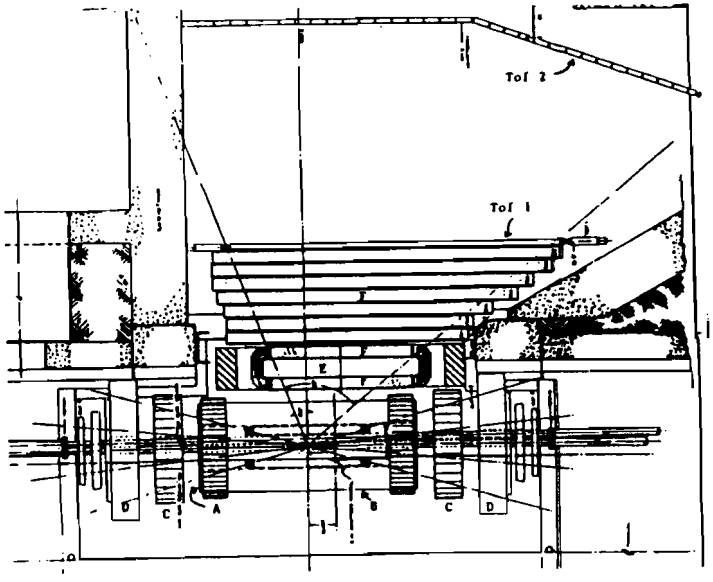

A = central chamber
B = barrel hodoscope
C = end cap chambers
D = end cap hodoscopes
E = magnet
F = 90° spectrometer chambers

Figure 6 - Plan view E735 detector.

Charged particles with a pseudo-rapidity magnitude of less than 3 will be detected in a cylindrical drift chamber. 60 tracks will be detected and measured in an event containing 100 charged particles distributed uniformally in pseudo-rapidity. The chamber is designed to detect up to 125 tracks in a single event. Since this chamber is not immersed in a magnetic field the momenta of the charged particle tracks and hence the rapidity cannot be measured. The pseudo-rapidity of each track can be calculated from its measured direction.

A magnetic spectrometer, which has an acceptance of 20° in azimuth and 1.35 units of pseudo-rapidity, is used to measure the momenta of at least one charged particle per recorded event. One class of event trigger will require a charged particle to traverse the spectrometer. The experimenters assume that the P_T of this particle will be proportional to the average energy per degree of freedom in the plasma. They will measure the $dNc/d\eta$ in the interval $|\eta|<3$ and the momenta of at least one charged particle. They will also determine whether the particle transversing the magnetic spectrometer is a π, K or p by means of time of flight. Since $\beta*$ at CØ is 75 m the luminosity will be about 10^{28} cm^{-2} sec^{-1}. Such a luminosity is compatible with the experimenters needs.

The installation of the experiment is in progress. It should be ready to take data toward the end of the collider run although the central track chamber may not be completed until the start of the second collider run.

In certain respects a large general purpose detector such as CDF can also detect the events of interest to E735 because it can be used to measure charged particle momenta and γ ray energies in the pseudo rapidity interval of ± 4. It can distinguish e's, μ's, and hadrons from one another and it can also detect K_S^0's through

$\pi^+\pi^-$ decay. The CDF luminosity monitor, which consists of series of segmented silicon counter telescopes located on either side of the interaction region in a manner similar to E710 can measure the multiplicity of particles emitted in the very forward and backward regions. The segmented silicon wafers are arranged so that the multiplicity can be measured over the pseudo rapidity interval of $6<|\eta|<8$. A specific objective of this hardware is to trigger on diffractive events and measure the character of the rapidity distribution of these events using the central detector to observe the central 8 units of rapidity. Nevertheless for CDF to make measurements like those of E735 the solenoid field would have to be reduced significantly, the luminosity reduced by increasing β^* to 100m, and a special trigger developed. The CDF group would also have to dedicate a significant allocation of their running time to this physics, at the cost of doing less of their original objectives. For the moment there is room for the small experiments in the shadows of the giants.

CDF and DØ Detectors

The physics objectives of CDF and DØ are similar in that both groups are searching for new physics above the W and Z production thresholds. Both detectors are designed to observe the products of hard collisions of a gluon or quark in the proton with a gluon or quark in the antiproton. Since the differences in the detectors distinguish the physics goals of the two groups, I will begin by briefly describing the detectors.

Collider Detector At Fermilab (CDF)[8]

A schematic of half of CDF is shown in the Figure 7.

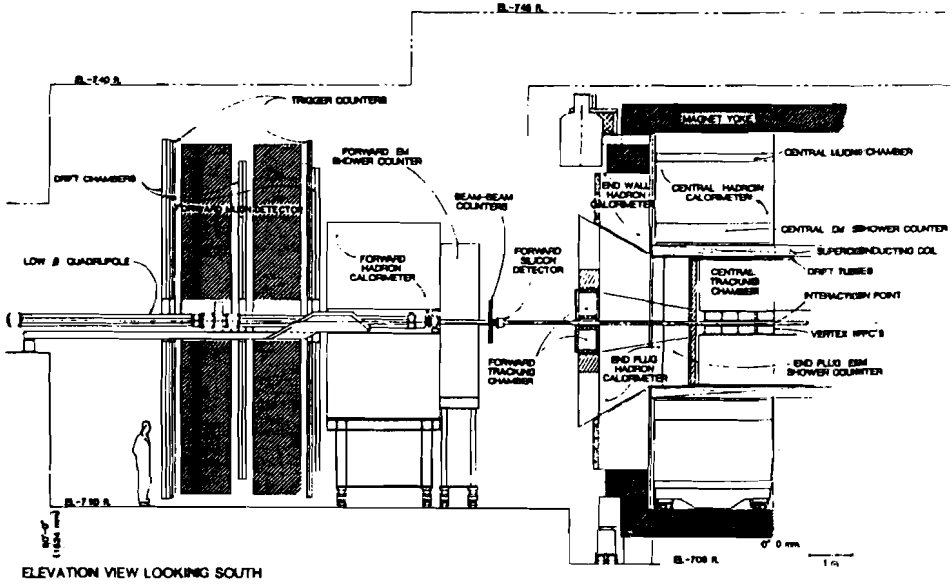

Figure 7 - A view of the west half of CDF. The detector has reflection symmetry about the plane perpendicular to the paper containing the interaction point.

The central detector consists of a 3m diameter, 1.5T solenoid filled with track chambers. The momentum of a charged particle can be measured provided the angle the charged particle makes with the beam is greater than about 20°. The solenoid is surrounded by a set of seven segmented calorimeters. The central calorimeter, the end wall calorimeters, and the end plug calorimeters nestle together as part of the central detector. The forward and backward calorimeters, which are separately installed complete the array. Since the largest angle that a particle can subtend with respect to the beam and escape detection by all of the calorimeters is 2°, the acceptance of the calorimeters is ±4 units of rapidity. The segmentation, or

element size, is 5° in azimuth and .1 units of rapidity for all calorimeters elements except those in the central calorimeter. These have a segmentation of 15° in azimuth and .1 units of rapidity.

A summary of the characteristics of the CDF calorimeters is given in Table 6.

Table 6: CDF CALORIMETERS

ELECTROMAGNETIC CALORIMETERS

	CENTRAL	PLUG	FORWARD
Sampling Medium	Scintillator	Gas	Gas
Thickness	$17X_o$	$19X_o$	$24X_o$
1/2 Angular Range	36°-90°	10°-37°	2°-10°
Element Size ($\delta\theta x\delta\eta$)	15° x .1	5° x .1	5° x .1
$\sigma_E/\sqrt{E}$	.15	.25	.25
Hadron Rejection	10^3	$5x10^2$	$2.5x10^2$

HADRON CALORIMETERS

	CENTRAL	WALL	PLUG	FORWARD
Sampling Medium	Scintillator	Scintillator	Gas	Gas
Thickness	$5X_c$	$4.4X_c$	$6X_c$	$8.3X_c$
1/2 Angular Range	40°-90°	30°-50°	10°-30°	2°-10°
Element Size ($\delta\theta x\delta\eta$)	15° x .1	15°x .1	5°x .1	5° x .1
$(\sigma_E)/\sqrt{E}$	(0.75)	.90	1.00	1.00

Electrons and γ's deposit essentially all of their energy in the electromagnetic calorimeter, and hadrons deposit on average about one third of their energy in electromagnetic calorimeter and the remainder in the hadron calorimeter. The ratio of the energies deposited in the two types of calorimeters is used to distinguish electrons from charged pions, when only a single charged particle traverses a calorimeter cell. Typically single hadrons are rejected by a factor of 300 to 1000 with this technique.

The CDF detector has track chambers located outside of the calorimeter to measure the direction of penetrating charged particles, such as muons. Downstream of the forward and backward calorimeters, magnetized iron toroids and track chambers are placed to detect muons. Between 17° and 50° (and 163° and 130°) there are no muon chambers.

DØ Detector[9)]

The DØ detector is shown in Figure 8.

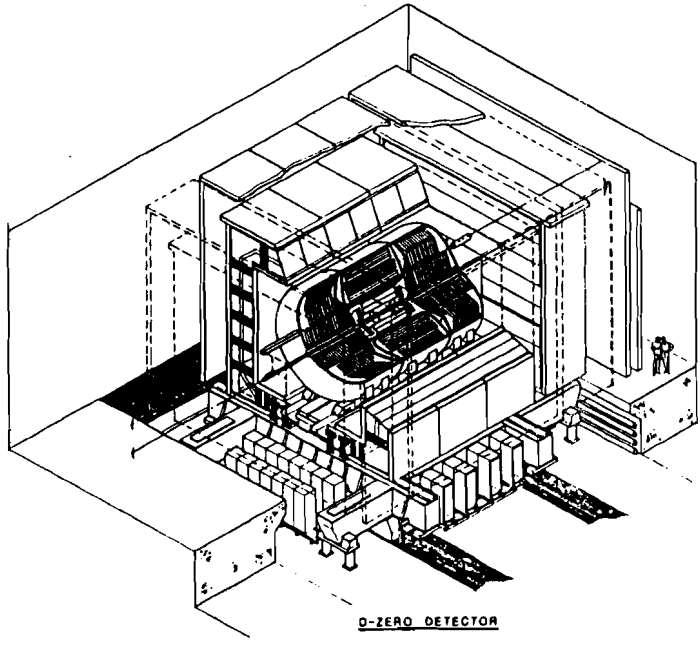

Figure 8

The beam pipe is surrounded by track chambers which are not immersed in a magnetic field. This is the first important difference between DØ and CDF. The DØ calorimeter which surrounds the track chambers consists of three segmented ionization sampling calorimeters. The central calorimeter is

made "hermetic" by two endcap calorimeters as shown in Figure 8. The sampling medium is liquid argon and the radiator consists primarily of uranium plates. A summary of the properties of the calorimeters is given in Table 8.

Table 8: DØ CALORIMETERS

ELECTROMAGNETIC

	CENTRAL CALORIMETER	ENDCAP CALORIMETER
Sampling medium	Liquid Ar	Liquid Ar
Radiator material	U	U
Total thickness	20.5X0	20.5X0
Element size ($\Delta\theta x\Delta\eta$)	$5.7^{o}x.1$*	$5.7^{o}x.1$*
$(\sigma_E)/\sqrt{E}$	12%	12%
Hadron rejection	10^3	10^3

*At shower max the element size is $2.8^{o}x0.05$

HADRONIC

	CENTRAL CALORIMETER	ENDCAP CALORIMETER
Sampling medium	Liquid Ar	Liquid Ar
Fine radiator	U ($3.24X_i$)	U($3.24X_i$)
Coarse radiator	Cu	Cu
Total thickness*	$6.93X_i$	$6.93X_i$
Element size ($\Delta\theta x\Delta\eta$)	$5.7^{o}x.1$	$5.7^{o}x.1$
$(\sigma_E)/\sqrt{E}$	40%	40%

*Electromagnetic calorimeter included.

The choice of U and Cu for various radiators gives the calorimeter a response function which is nearly the same for electromagnetic showers and hadronic showers. The response function is the ratio of the charge collected per GeV of energy deposited. The ratio of the electromagnetic response to hadronic response was measured to be 1.1 to ±10% in tests of the DØ prototype calorimeter. The nearly uniform response function and the 7 interaction length depth are the principal reasons for the good energy resolution. The designers of the calorimeter believe that the systematic errors in energy measurements should be both small and correctable.

It is also worth noting that the 7 interaction lengths of uranium and copper make an excellent muon filter. To take advantage of that circumstance the calorimeter is surrounded by magnetized steel and track chambers. The track chambers are located between the calorimeter and the magnetized steel and outside of the magnetized steel. They measure the direction and momentum of each penetrating particle. Because a muon must transverse more than 8 collision lengths of uranium, copper, and steel before reaching the outermost muon chambers the probability of hadronic punch through is much smaller in the DØ detector than it is in the CDF detector. One other feature distinguishes DØ from CDF: the DØ detector uses a set of transition radiation detectors (TRD) interspersed with the tracking chambers to identify electrons in a cluster of hadrons.

The DØ and CDF detectors are designed to measure the direction and energy of hadrons, electrons, and γ rays over the rapidity interval of ± 4 units. The DØ detector is designed to detect muons over the same interval, whereas CDF detects muons only over a fraction of the full solid angle.

The Physics Objectives of CDF and DØ

The objectives can be subdivided into four rough categories as follows: tests of QCD at large Q^2, tests of the electroweak model, a search for heavy quarks (top and beyond), and a search for other new particles.

Tests of QCD at Large Q^2

Until jets were observed in UA-1 and UA-2 at the Sp$\bar{p}$S, data from hadron collisions at lower energy accelerators provided very little conclusive evidence in support of QCD.[10] Prior to the Sp$\bar{p}$S measurements even the observation of jets in low energy hadron collisions ($\sqrt{s}$<30) was controversial. Far more information came from lepton-nucleon scattering and e+e- collisions. Because jet transverse momenta of 500 GeV/c can be reached with the Tevatron there is an incentive to make qualitative tests of QCD at Q^2 which are beyond the kinematic limits of SLC, LEP or HERA. CDF and DØ intend to measure the two jet, three jet and multijet cross sections.

When the integrated luminosity of the Tevatron reaches 10^{37} cm^{-2} two jet events with transverse momenta of up to 500 Gev/c should be observed. A measurement of the two jet cross sections out to 500 GeV/c will probe the short distance structures of the quarks and gluons down to $4x10^{-17}$cm. Since QCD calculations of the shape of the inclusive $\bar{p}p$ jet cross section using the proton structure functions obtained from lepton nucleon scattering are in very good agreement with single jet data from the Sp$\bar{p}$S[11] a deviation from the predicted cross section at still higher Q^2 would indicate the threshold of phenomena beyond the standard model. It could for example reveal the presence of quark substructure.[12]

Careful measurement of the ratio of the symmetric three jet to two jet cross section will provide some qualitative information on the large Q^2 dependence of α_s. Since the DØ detector should be able to detect isolated γ's it should be possible for it to obtain a measure of the ratio of the (2 jet + γ) cross section to the 3 jet cross section in the kinematic region where the inclusive γ cross section is greater than π^o cross section. The

ratio of these two cross sections is proportional to α_{em}/α_s. While it is doubtful that the data from these detectors will be able to make quantitative tests of QCD because of the inherent difficulty of relating an experimentally defined jet to a quark or gluon, the data should be able to provide important qualitative information on the domain of validity of QCD.

Tests of the Electroweak Model

The CDF and DØ detectors will detect a very large number of W's and Z's. Because the total momentum of the proton and antiproton carried by the quark-antiquark pairs in the sea surrounding the valence quarks is large enough to produce W's, the production of these bosons is not restricted to the valence quarks. At the Tevatron weak boson production by annihilation of sea quarks is roughly as important as production by valence quark annihilation.[13] This is one of the reasons that the production cross section increases by a factor of 3.5 from $\sqrt{s}$=630 (Sp$\bar{p}$S) to $\sqrt{s}$=1800 (Tevatron).

For an integrated luminosity of $10^{37}cm^{-2}$ CDF and DØ should each detect 7,500 W^+s decaying to $e^+ + \nu_e$, 7,500 W^-'s decaying to $e^- + \bar{\nu}_e$ and 1,500 Z^o's decaying e+e−. The DØ detector will detect an equal number of muon decays of these bosons. The CDF detector will detect only 60% as many muon decays as electron decays with its current muon detection system. The CDF collaboration plans to increase the solid angle of the muon system in the future.

One of the goals of the DØ group is to simultaneously measure the mass and width of both the W and Z. From the ratio of the masses they hope to measure $\sin^2\theta_W$ to $\pm.0012$. CDF and the Sp$\bar{p}$S experiments will measure this quantity earlier, although with less precision.

Should the W and Z's be just the lightest members of a family of particles these detectors will be able to observe more massive W's and Z's decaying into leptons if their production cross section times branching ratio exceeds 10^{-36} cm^{-2}. If the coupling of these bosons to leptons and quarks is similar to those of the W and Z these heavier bosons will be detected if their masses are less than 500 GeV/c^2.[14]

Search for Heavy Quarks (Top and Beyond)

One of the striking features of the standard model is that the leptons and quarks can be grouped together in families. According to our current, nearly religious, belief each family consists of a lepton with charge +e, a neutrino with no charge, a quark with charge -1/3e, and a quark with charge +2/3e. While the charge 2/3 quark associated with the b quark has not been found theoretical particle physicists are sufficiently confident of its existence that they have already named it the top quark. If it exists its mass is certainly greater than 22 GeV since it has not been observed in e+e- collisions at PETRA. The CDF and DØ detectors as noted earlier have been designed to detect leptons in the presence of hadron jets. Thus they should be able to detect the semileptonic decays of the top quark if its mass is greater than 45 GeV/c^2 and less than 90 GeV/c^2. The lower limit is a consequence of the difficulty of separating semileptonic top decays from the very large background of semileptonic bottom decays. It is not a hard limit it should be possible to lower the limit somewhat by increasing the size of the sample events thereby making it possible to restrict the event kinematics to the most sensitive configurations. Given the complexity of the events and the background roughly 100 events with favorable kinematics are probably needed to make a discovery. The upper limit is consequence of a cross section which diminishes rapidly as the mass increases.

If the mass of t quark is less than 45 GeV than gluon fusion will be the dominant production mechanism. If the mass is below 45 GeV the top will be detected most readily in Z° decays at e^+e^- colliders. If the t quark mass is between 45 and 75 GeV then the dominant production mechanism for top quarks will be through production of W's and the subsequent decay into t and a b. The b jet from the W decay will have a transverse momentum between 8 GeV/c and 30 GeV/c. If the t quark decays semileptonically into a charged lepton, a neutrino and a b quark, which manifests itself as a second jet, then detectors such as CDF and DØ can distinguish these decays from others processes when the decay kinematics are favorable. Because there are at least two jets in the event there is a likelihood that the lepton from the top decay will tend to be mixed in with some of the hadrons from one or both of the jets. If the lepton from t decay is a muon then it will easily penetrate eight absorption lengths of material and reach the muon chambers. The hadrons in the jets will be absorbed in the calorimeter. The muon momentum will be measured to 20%, which should be adequate for measuring its transverse energy to a few GeV.

Another important ingredient in identifying these events is the fact that the there can be 10 or more GeV of missing transverse energy due to the undetected neutrino. This should be useful in identifying the top quark if it is more massive than 45 GeV. If the top quark mass is significantly less than 45 GeV the transverse momentum of the neutrino will only rarely be greater than 10 GeV. If transverse energy carried by the neutrino is less than 10 GeV it will be indistinguishable from fluctuations in the apparent energy imbalance caused by errors in the measurement of the transverse momentum of the hadrons and the charged leptons and the unobserved transverse momentum of the hadrons escaping down the beam line. Although this method off

analysis has been used by UA-1 to analyze Sp$\bar{p}$S data, no clear signal has been seen.[15] A result may emerge when higher statistics experiments are done at the Tevatron. Of all of the detectors under construction the DØ detector should have the greatest sensitivity to missing transverse energy.

If the top mass is greater than 83 GeV then the only significant production mechanism will be gluon fusion. Under these circumstances it will be more likely to find the top quark at the Tevatron than at Sp$\bar{p}$S because of the larger cross section for top quark production by gluon fusion. CDF and DØ should be able to detect the quark if its mass does not exceed 90 GeV/c^2 and if the integrated luminosity reaches $10^{37}cm^{-2}$. Under these circumstances 100 events should be detected. If the top mass is between 22 and 30 GeV it should be seen at Tristan, SLC, and LEP.

Search for New Particles

Since new physics is by definition unpredictable. I will leave it to the future to judge whether the CDF and DØ detectors are capable of detecting the new physics which will hopefully be within our reach. Perhaps a number of surprises will be offered by the Tevatron when CDF and DØ begin to observe constituent collisions with 500 GeV of energy.

Certainly we should all know a lot more about the top in two years time when the results begin to emerge from all the new accelerators as well as the improved ones.

Acknowledgments

I wish to thank Paul Grannis, Carlos Hojvat, Hans Jensen, Roy Rubinstein, and Frank Turkot for providing materials on the detectors.

References

1. Design Report, Tevatron I Project, September 1984, (Fermilab), J. Peoples, "The Fermilab Antiproton Source", IEEE Trans. Nucl. Sci., Vol. NS-30, p. 1970 (1983). R. Shafer, "Overview of the Fermilab Antiproton Source", Proc. of the 12th Intl. Conf on High Energy Accelerators, p. 24, (1983). G. Dugan, "Tevatron I: Energy Saver and $\bar{p}$ Source," IEEE Trans. Nucl. Sci., Vol NS-32, p. 1582 (1985). S. Holmes, "Initial Operation of the Fermilab Antiproton Source", Proc. of the Oregon Meeting - Division of Particle Fields, p. 949 (1986).

2. S. van der Meer, "Stochastic Cooling of Betatron Oscillations in the ISR", CERN/ISR-PO/72-31, CERN (1972). A more complete description of the principle of stochastic cooling is given in D. Mohl, G. Petrucci, L. Thorndahl, and S. van der Meer, "Physics and Techniques of Stochastic Cooling", Phys. Rep. 58,73.

3. H. Edwards, "The Fermilab Tevatron and Pbar Source Status Report", Proceedings of the 13th International Conference on High Energy Accelerators, Novosibirsk (1986).

4. Since this manuscript was prepared, colliding beams were reestablished in the Tevatron at a center of mass energy of 1800 GeV.

5. M. Bozzo, et al., Phys. Lett. 147B, p. 392 (1984).

6. F. Turkot, $\bar{p}p$ Searches for Quarks-Gluon Plasma at Tev I, "Quark Matter 86", Asilomar, Ca., (1986). C. Hojvat, "Antiproton Proton Searches for Quark-Gluon Plasma at the Fermilab Collider", Fermilab-Conf 86/137.

7. L. Van Hove, Phys Lett. 118B, 138 (1982).

8. H. Jensen, "The Collider Detector at Fermilab (CDF)", IEEE Nucleon Science Symposium, San Francisco (1985). M. Eaton, "Status of CDF", Sixth Topical Workshop on Proton-Antiproton Collider Physics, Aachen (1986), preprint. M. Marx, "Status of the DØ Detector", Sixth Topical Workshop on Proton-Antiproton Collider Physics, Aachen (1986), preprint.

9. M. Eaton, "Status of CDF", Sixth Topical Workshop on Proton-Antiproton Collider Physics, Aachen (1986), preprint. M. Marx, "Status of the DØ Detector", Sixth Topical Workshop on Proton-Antiproton Collider Physics, Aachen (1986), preprint.

10. M. Banner, et al (UA2 collaboration), Phys. Lett. 118B, 203 (1982), G. Arnison et al (UA1 collaboration), Phys. Lett. 123B, 115 (1983), more recent measurements are included in the following: G. Arnison et al (UA1 collaboration), Phys. Lett. 136B, 294 (1984), P. Bognaia, et al (UA2 collaboration), Phys. Lett. 144B, 283 (1984), W. Scott, "Jet Production and QCD in the UA1 Experiment", Proceedings of the International Symposium on Physics of Proton-Antiproton Collision, p. 68, Tsukuba (1985).

11. D. Froidevaux, "Latest Results on High P_T Jets in UA-2", Proceedings of the International Symposium on Physics of Proton-Antiproton Collision, p. 97, Tsukuba (1985).

12. E. Eichten, "Theoretical Expectations at Collider Energies", Fermilab-Conf-85/178-T, p. 169 (1985).

13. E. Eichten, "Theoretical Expectations at Collider Energies", Fermilab-Conf-85/178-T, p. 73, (May, 1986).

14. E. Eichten, "Theoretical Expectations at collider Energies", Fermilab-Conf-85/178-T, p. 95, (May, 1986).

15. M.N. Minnard, "Associated Productino of Lepton and Jets", Proceedings of the International Symposium on Physics of Proton-Antiproton Collision, p. 409, Tusukuba (1985).